nature energy

Article

https://doi.org/10.1038/s41560-023-01315-7

A socio-technical approach for the assessment of critical infrastructure system vulnerability in extreme weather events

Received: 25 October 2022

Accepted: 28 June 2023

Published online: 31 July 2023

Check for updates

Juan P. Montoya-Rincon [1] ✉, Said A. Mejia-Manrique [2] ✉, Shams Azad [3], Masoud Ghandehari[3], Eric W. Harmsen [4], Reza Khanbilvardi[2] & Jorge E. Gonzalez-Cruz [1,5]

The recurrence of extreme weather events has led to the development of methods for assessing the vulnerability and interdependencies of physical and human systems. A case example is Hurricane Maria (H-Maria), where Puerto Rico experienced damage to 80% of its electrical power system, leading to massive disruptions of essential services for months. Here we evaluate the effectiveness of various interventions aimed at reducing vulnerability by considering power and water infrastructure and respective water–power dependencies while also considering the social vulnerability of affected communities associated with the physical infrastructure upgrades. On the basis of the current infrastructure configuration, we found that all communities suffered enormously from power and water outages. As one upgrade option, we show that incorporating regional energy grids would reduce outages in an H-Maria scenario. However, a large portion of disadvantaged communities will face service disruption under this option. In contrast, hardening transmission lines, as the second option, would improve service delivery and, most importantly, provide uninterrupted service to the higher portion of the vulnerable population.

Hurricanes are notorious for wreaking havoc on critical infrastructure through strong winds and floods[1], causing damage that translates to people losing power and substantial disruptions of essential services, such as drinking water, food supply, access to medical treatment and communications. For instance, in the case of Hurricane Sandy (2012), nearly 2,500 transformers and more than 4,400 distribution poles were left damaged in its passage through Long Island, New York, causing the loss of power to 90% of Long Island Power Authority's customers[2]. Considerable damage to the critical infrastructure was also experienced in numerous New York communities, resulting in water scarcity for two to three weeks[3].

A more recent example, Hurricane Maria (H-Maria), which made landfall in Puerto Rico on 20 September 2017, as a high-end category 4 hurricane[4], severely damaged over half of the transmission towers and 50,000 of the distribution poles in Puerto Rico[5], leaving the island with a near-complete blackout. After one month, less than 20% of the overall power capacity of the island was restored[6].

Risk mitigation planning is often carried out in the aftermath of such failures. In most cases, they concentrate on strengthening particular system components of the affected critical infrastructure[7,8]. The focus is often on overall service delivery improvements[9], subject to physical cost constraints. After H-Maria, two system upgrade options

[1]Department of Mechanical Engineering, The City College of New York, New York, NY, USA. [2]Department of Civil Engineering, The City College of New York, New York, NY, USA. [3]Department of Civil and Urban Engineering, New York University, Brooklyn, NY, USA. [4]Department of Agricultural and Biosystems Engineering, University of Puerto Rico, Mayaguez, Puerto Rico, USA. [5]Department of Atmospheric and Environmental Sciences, University at Albany, Albany, NY, USA. ✉e-mail: jmontoyarincon@ccny.cuny.edu; smejiamanrique@ccny.cuny.edu

received popularity among policymakers to reduce the vulnerability of the power delivery of the island[10]. The first option was the hardening of transmission lines. This upgrade focuses on enhancing the transmission system by either a targeted hardening of structures[11] or burying the lines[1]. The second option was switching from centralized to decentralized power generation using mini-grids[12,13].

Infrastructure interdependencies exist in most instances; for example, the water distribution supply heavily depends on power delivery[14]. In other words, reducing the vulnerability of the power network improves both power delivery and water supply. A number of other studies have highlighted the importance of understanding how the vulnerability of one system can impact the other, for example, through an analysis of the interdependency between power and water infrastructures[15,16]. Water infrastructures rely on power to extract, treat and distribute water for residential, commercial, irrigation and industrial uses[15]. Power systems rely on water to cool the power generators or generate energy, such as thermoelectric generation and hydropower. Additionally, critical power and water systems may be susceptible to flooding events, with cascading effects, threatening human well-being and often with important economic damage[17].

In a disastrous event such as a hurricane, communities have varying degrees of physical vulnerability concerning water and power infrastructure services[18]. Social vulnerability of a community is a metric often used to express the extent and/or nature of response and recovery from the disaster[19–21]. It is defined as the capacity of a person or group to prepare for and be faced with the adverse impacts of natural hazards, which involves a combination of factors determining the degree to which a person's life and belongings are put at risk[22]. Over the last 40 years, social vulnerability to disasters has grown its attention in a way to describe the interaction between social inequality and the impact consequences associated with disasters relating to the disparate distribution of susceptibility to harm[23]. It is now widely accepted that to reduce community vulnerability and lessen suffering, it is crucial to consider social vulnerability when designing and implementing policies[24–26].

In this study, we present a methodology to assess the social vulnerability of extreme events with high resolution. We apply it to the case example of H-Maria. Considering power and water infrastructure and respective water–power dependencies, we evaluate the effectiveness of various interventions aimed at reducing vulnerability. We consider the societal consequences of physical infrastructure upgrades through a system-level vulnerability analysis approach, which may be used to support decision-making.

Modelling of the power infrastructure

This study used western Puerto Rico as the test area. Figure 1a shows the island as an insert and the elevation map of western Puerto Rico, delineating the eight counties (municipalities/municipios) used in the analysis.

To quantify the effect of hurricanes on critical infrastructure and services (power and water), we first estimate the damage to the electrical power transmission towers, then quantify the damage in each transmission line and subsequently use this information along with a power network model to estimate the number of people impacted.

The first element of the analysis is the transmission service level. A model used to estimate the failure in the transmission towers uses the type of structure, the material of the tower and weather conditions at that specific location (wind speed and precipitation) to make predictions. We used the Power Tower Failure model (PTF), proposed by Montoya et al.[27], which is a machine-learning model that was trained on damaged reports provided by Puerto Rico Power Authority and is able to estimate the damage to a power tower given weather variables, such as wind speed and precipitation. Damage reports provided by the utility agency provided information on the location, material, type and level of damage after H-Maria for the power towers on most of the transmission lines.

The Power Network Model (PNM)[28] is then used as the second component of the analysis. This network model incorporates all the generation centres and transmission lines in Puerto Rico. Furthermore, the PNM uses a list of failed transmission lines as input to estimate people without power in a county-scale resolution. Specifically, to calculate the level of damage to each transmission line, the PTF's output is utilized by predicting the damage in the transmission structures and aggregating the result on a line-by-line basis. Moreover, the transmission lines with more than 1% of their towers damaged are reported as failed in the PNM input. This threshold was selected by running the coupled models and validating the PNM results with H-Maria data.

While the PNM, at the county-scale resolution is useful, a finer spatial resolution is needed for a more in-depth analysis of human impact. Consequently, we downscaled the PNM output using the 500 m-resolution space-borne nightlight imagery product (NTL) from the National Aeronautics and Space Administration (NASA)[29]. This product was proven to be a more accurate representation of the spatial distribution of power loss induced by H-Maria on the island[30–33]. Figure 1b–e shows the power service level immediately after H-Maria, at county and county subdivision (barrios) resolution, and the average daily pre-hurricane water demand ($m^3\ d^{-1}$) per customers at the two resolutions. When a county's electric power goes out, we use the nightlight data to model the county's subdivision. If a county's power (using the utility company record) does not go out, we assume the same for the county subdivision.

Modelling of the water infrastructure

A Water Distribution Model (WDM) was developed based on a preliminary detailed water distribution model built by the Puerto Rico Aqueducts and Sewers Authority (PRASA) for eight counties in western Puerto Rico using the hydraulic modelling software InfoWater[34]. These counties included Añasco, Aguada, Aguadilla, Hormigueros, Isabela, Mayagüez, Moca and Rincón (Fig. 1a). The WDM junction demands were updated using the internal PRASA report on the customer demands and their location near each junction. Figure 1d,e shows the average daily demand ($m^3\ d^{-1}$) of the customers for county and county subdivisions, respectively.

It should be noted that there were also back-up generators of the water pump stations. Those generators that were functioning were incorporated into the potable water distribution simulations. Potable water pump facilities located in the counties of Aguadilla, Hormigueros and Rincón lacked back-up generators when the event occurred. Other counties had partial access to back-up generation. These included the counties of Aguada (5%), Añasco (32%), Isabela (30%), Mayagüez (14%) and Moca (17%).

Flood modelling

Extreme weather events such as hurricanes and the accompanying high winds and flooding[1,35] are responsible for the loss of human life and costly damage to critical infrastructure. To quantify flooding, several hydrologic models have been developed for different watersheds in Puerto Rico, such as MIKE SHE, Vflow and the Gridded Surface Subsurface Hydrologic Analysis[36] (GSSHA) model[37–39]. Prior authors[35] found that the GSSHA model has great potential to reconstruct or forecast flooding events if properly calibrated and validated to produce a reasonable streamflow estimate and to identify flooding during extreme weather conditions. In this study, the GSSHA software was used to build a hydrologic model with the aim of simulating the flooding depth and extent during H-Maria and finding which water and electrical infrastructure might be affected by flooding. The four largest watersheds used were the Añasco, Culebriñas, Guanajibo and Yagüez watersheds, with an approximate area of 548, 335, 393 and 42 square kilometres, respectively. The methodology described by Mejia-Manrique et al. for Añasco was employed to develop the remaining hydrologic models of Culebriñas, Guanajibo and Yagüez watersheds[35]. It should be

https://doi.org/10.1038/s41560-023-01315-7

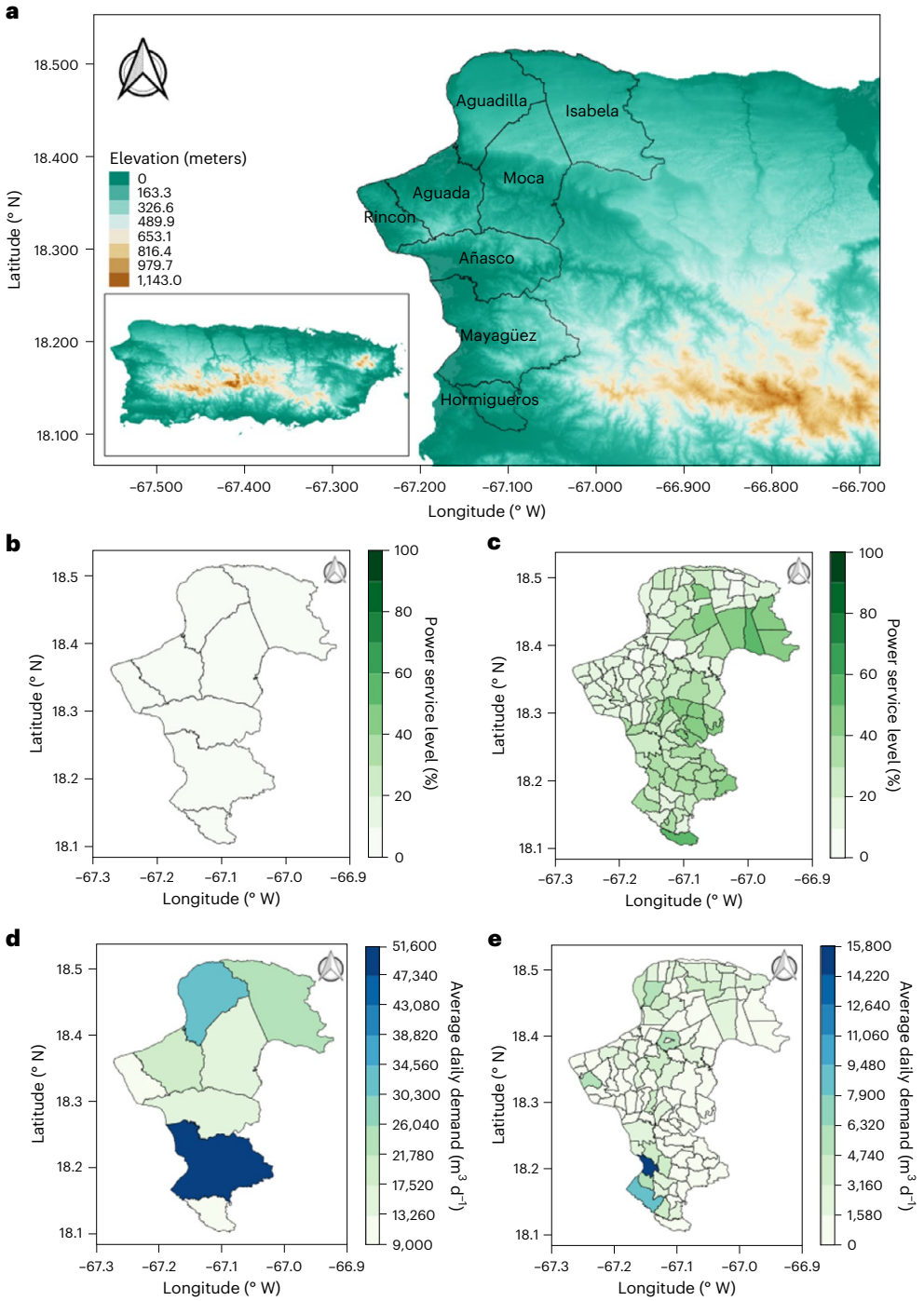

Fig. 1 | Study area and downscaled model results in the aftermath of H-Maria. We choose 22 September 2017 as the date for analysis. **a**, Overall study area, western Puerto Rico. The inset shows the island of Puerto Rico with the elevation contours. **b**, Power service level at county resolution. **c**, Power service level at county subdivision resolution. **d**, Average daily pre-hurricane water demand ($m^3\ d^{-1}$) for customers per county. **e**, Average daily water demand ($m^3\ d^{-1}$) for customers per county subdivision.

mentioned that the calibration and validation processes were done for only Culebriñas and Guanajibo watersheds because these two watersheds have a United States Geological Survey (USGS) stream discharge station.

Moreover, it should be noted that the results generated by Mejia-Manrique et al. for the Añasco watershed were used in this study. Due to the close proximity and similarity in the most representative land-use land cover and soil-type classes, we assumed the calibrated parameters for the Yagüez watershed to be the same as the Añasco. The performance of the hydrologic models was evaluated by verifying that the coefficient of determination (R^2) would be greater than 0.6 and the Nash–Sutcliffe efficient (NSE) greater than 0.5 between the simulated and the observed discharge at the USGS discharge station[40]. As a result, the evaluation criteria were achieved for the calibration and validation process for the different watersheds (Table 1).

The weather surveillance radar (WSR-88D) instrument in Puerto Rico was destroyed during the passage of H-Maria[4]. Therefore a bias-corrected rainfall model from Mejia-Manrique et al.[35] was used to simulate the flooding event on the watersheds of the coastal areas. Coastal areas had the highest impacts by floods due to the high

Table 1 | Performance of the hydrologic models for the calibration and validation of the hydrologic parameters

Calibration rainfall events			
Watershed	**Rainfall events**	**R^2 > 0.6**	**NSE > 0.5**
Añasco	September 06th (16:00) – 08th (15:00) of 2017 GMT[a]	0.61	0.55
Culebriñas	November 12th (20:00) – 14th (22:00) of 2016 GMT	0.95	0.85
Guanajibo	September 06th (16:00) – 08th (15:00) of 2017 GMT	0.89	0.58
Validation rainfall events			
Watershed	**Rainfall Event**	**R^2 > 0.6**	**NSE > 0.5**
Añasco	11 December (04:00)–13 December (04:00) 2007 GMT	0.95	0.9
Culebriñas	20 August (12:00)–22 August (14:00) 2017 GMT	0.9	0.9
Guanajibo	11 December (04:00)–13 December (04:00) 2007 GMT	0.83	0.51

[a]Greenwich Mean Time.

discharge and extensive river meandering. Figure 2 shows the flooding results for the four watersheds mentioned. Subsequently, it was found that four and six potable water pump stations of the WDM in Añasco and Guanajibo might have been impacted by flooding during H-Maria. In addition, the only transmission centre located within the study area (precisely in the Añasco watershed) was unaffected by the flooding results.

Integrated scenarios

A variety of solutions for decreasing the grid vulnerability have been suggested after H-Maria's devastating damage to the island. In this study, we focus on the baseline infrastructure scenario and two scenarios with upgrades to the power infrastructure. The first upgrade option is the *hardening of the transmission lines*. Hardening of the transmission system as an aid to the vulnerability in extreme weather events has been suggested in different studies[41,42]. In the context of H-Maria, we focus on the hardening of the transmission towers on the 115 kV lines (Fig. 3a). In Puerto Rico, these lines are mostly comprised of two-pole and single-pole structures made from wood. Moreover, wooden structures are usually the most fragile components in the transmission system. Montoya et al. proposed replacing the wooden structures with more resistant steel self-support poles[27]. The authors found that by upgrading the system, there would be an average improvement in the percentage of damaged structures of 10% in all the transmission lines and a maximum improvement of 66% in one of the lines. Following their findings, the replacement was carried out in the PTF, specifically by replacing all the wooden structures in the 115 kV lines with steel self-support poles. In this study we use these hardening benefits as input to the PNM, allowing us to examine the effects of transmission lines upgrades on the power and water delivery (Fig. 4).

The second upgrade considered the implementation of mini-grids. The term *mini-grids* refers to a decentralized power generation and distribution system where the area of interest is divided into different self-contained load islands that work as a coupled system but are capable of decoupling in case of failure. Furthermore, mini-grids and micro-grids have been popular options to increase renewable energy penetration and reduce the vulnerability in extreme events[12,43,44]. On the basis of the 2019 proposed *Puerto Rico Integrated Resource Plan*[45] (IRP), eight mini-grids would be incorporated into PR. To integrate this option into our study, we added the corresponding generation centres to the power network model, connecting them to the closest existing node. The new generation centres along with the mini-grids are shown in Fig. 3a. The impact of the additional mini-grids will be compared with the baseline infrastructure and the lines hardening upgrade (option 1 described above) to determine which solution is more effective in terms of power (Fig. 5b,c), water (Fig. 5e,f) availability and social impact.

Power–water coupling

Inspired by previous studies[46,47], we address the power–water system dependency solely through the electrical power consumed by the water pumps due to the lack of water facilities that generate electricity in the study area, such as hydropower. We assume a centralized pump power source at the county level. For instance, if the output of the power network model indicates that a county will not have power, it will turn off all the pumps within that specific county, keeping only the ones with back-up generators. Figure 3b shows how the electrical connection of the pumps and the centroid of the PNM model per county were assumed. It should be mentioned that all intake facilities of the water distribution model, such as filtration plants, reservoirs, dams, water treatment plants for potable water and wells, were assumed to be in continuous operation, which means that they had a generator that provided electricity during the event in case of having power outages. Moreover, the potable water pump stations affected by flooding were turned off in the WDM. However, some of those pumps affected by flooding served a small population, so there were no apparent changes in service level in the county subdivisions. For other pumps, water pressure was reduced, so people could get water but at low pressure. Finally, the PNM and WDM models were run in a steady state for each of the scenarios and an analysis of the extent of their service loss was modelled to quantify the vulnerability of the existing water and power infrastructure (Fig. 5a,d).

Socio-technical analysis

During extreme events, the disruptions in service delivery of critical infrastructures disproportionately impact communities based on socioeconomic and demographic characteristics[48]. The Cutter social vulnerability index 2003 (SOVI) and the Centers for Disease Control and Prevention social vulnerability index 2011 (CDC SVI) are commonly used vulnerability indexes[49]. The Cutter SOVI uses 42 variables to assess vulnerability before factor analysis is applied to reduce dimensionality[50]. Meanwhile, the CDC SVI is more concise, utilizing only 15 variables and constructing the index using percentile ranking[19]. However, it's important to note that not all variables used in the two indexes are relevant during critical service outages.

To assess the social vulnerability of communities during critical service disruptions, we developed a social vulnerability index for Power and Water Service disruption (Sd-SVI). This index builds on the Centers for Disease Control and Prevention's Social Vulnerability Index (CDC SVI) by incorporating vulnerability indicators such as socioeconomic status (SES), household composition (HH) and accessibility, which are highly relevant for understanding vulnerability during power and water service disruptions.

Under the SES theme, we included attributes such as poverty, income, education and unemployment. Communities with lower SES are less likely to have the resources necessary to prepare for and recover from disasters, making them more vulnerable[50,51]. During power and water infrastructure failure after a disaster, they are also less likely to have access to alternate power sources such as generators or to purchase fuel and bottled water, making them more vulnerable to service disruptions[52]. The second theme, HH, includes features from the household composition. Researchers have established that dependent children under 18 years of age, people over 65 years, single-parent households and the disabled population increase the community's vulnerability by increasing the burden of care[50]. Older adults and children who rely on electricity-dependent medical equipment are particularly vulnerable to power outages[48]. Single-parent households are also at

https://doi.org/10.1038/s41560-023-01315-7

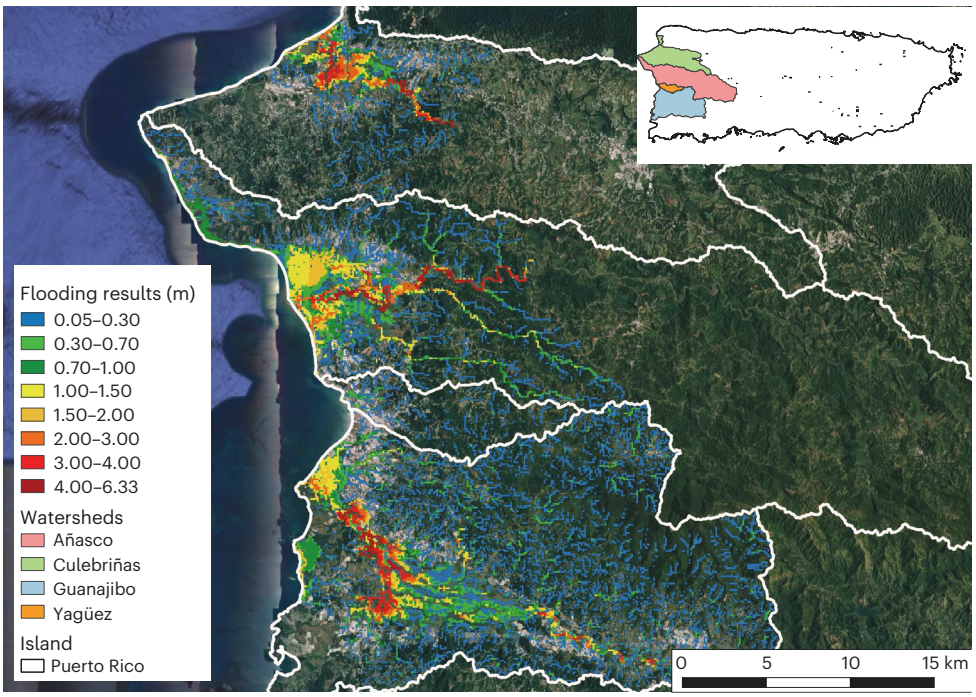

Fig. 2 | Flood modelling results. Results of flood modelling for the Añasco, Culebriñas, Guanajibo and Yagüez watersheds during H-Maria. The inset shows the location of the watersheds in the island of Puerto Rico.

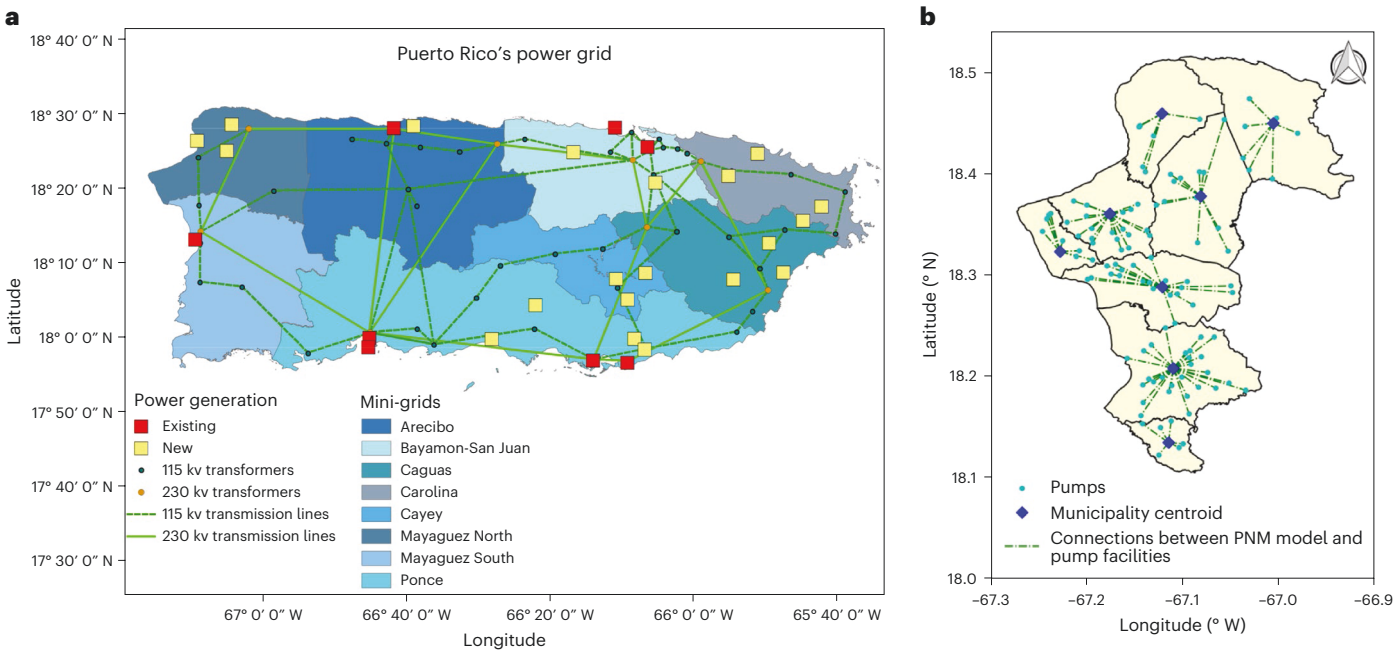

Fig. 3 | Power grid and water network pump in Puerto Rico. a, Mini-grids and new power generation centres (based on the Puerto Rico Integrated Resource Plan[45]). **b**, Assumption of the electrical connection of the pumps per county with the county centroids of PNM.

higher risk during disasters, as all the daily care responsibilities of the children fall on one parent. It can be challenging for that parent to provide their child with all the necessary supplies during a power or water outage.

In the Sd-SVI, in addition to the SES and HH themes, we incorporated a new theme focused on accessibility. This theme recognizes the importance of accessibility to crucial supplies and facilities during water and power outages. Under this theme, we included four attributes: road density, access to supermarkets and hospitals, and availability of private vehicles. Past studies have indicated that the density of roads is an essential factor in determining the overall accessibility of an area during extreme events. Locations with high road density tend to have a greater likelihood of having alternative routes available in case the primary roads become blocked due to landslides or floods caused by hurricanes[32]. Access to supermarkets facilitates getting necessary supplies in the event of outages in critical service. By utilizing their existing inventory, supermarkets can offer initial assistance to the community before external aid arrives in the area.

https://doi.org/10.1038/s41560-023-01315-7

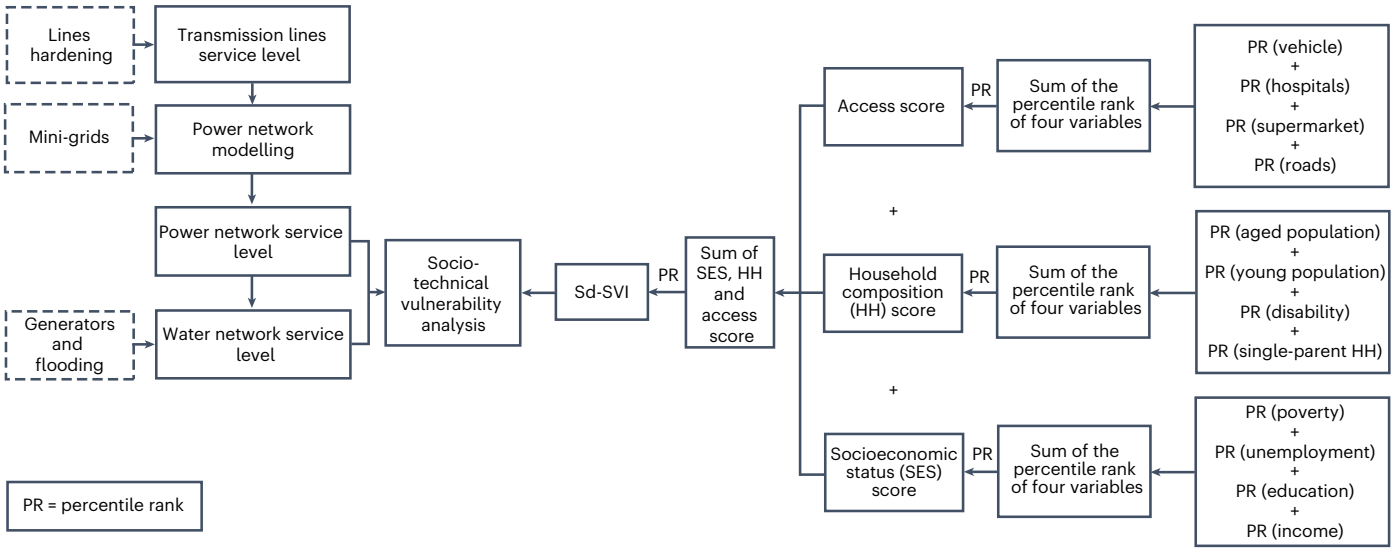

Fig. 4 | General framework. Socio-Technical Vulnerability Analysis flowchart, showing the power–water coupling and social vulnerability index for Power and Water Service disruption (Sd-SVI). The upgrades to the power infrastructure are shown in dashed lines.

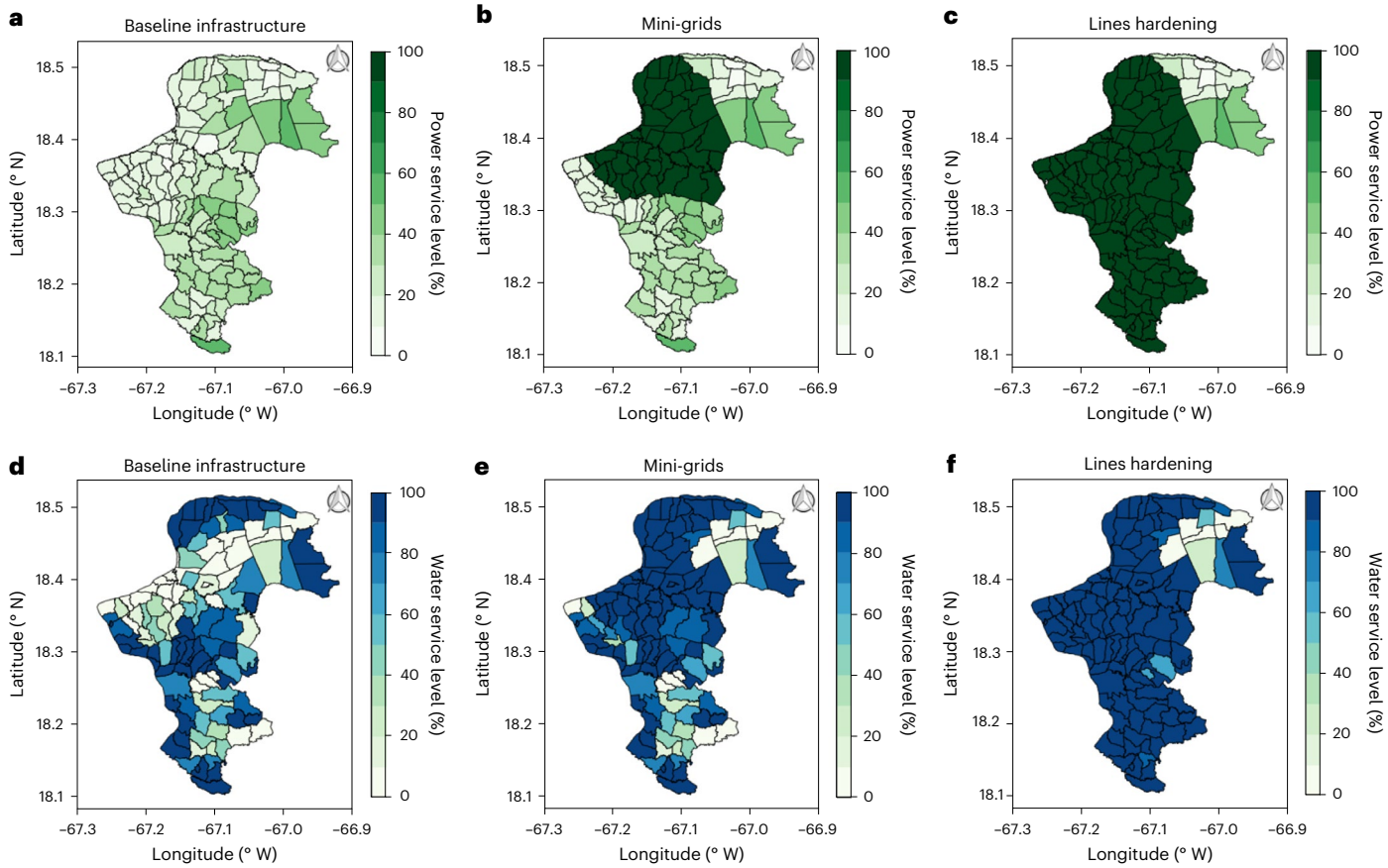

Fig. 5 | Results of the power and water models, shown as service level. a, Power service level in the baseline infrastructure scenario. **b**, Power service level in the mini-grids scenario. **c**, Power service level in the transmission lines hardening scenario **d**, Water service level in the baseline infrastructure scenario. **e**, Water service level in the mini-grids scenario. **f**, Water service level in the transmission lines hardening scenario.

Again, access to hospitals is vital because water service disruption frequently results in waterborne illnesses. For instance, unsafe drinking water after H-Maria caused waterborne diseases such as Leptospirosis, resulting in over 51 fatalities[53]. Also, during power outages, it is crucial to prioritize the transfer of patients to hospitals that rely on electricity-dependent medical equipment primarily used at home. Furthermore, households without vehicles are especially vulnerable because they cannot access necessary facilities and must rely on others for support. The description of the attributes in Sd-SVI are included in Methods.

https://doi.org/10.1038/s41560-023-01315-7

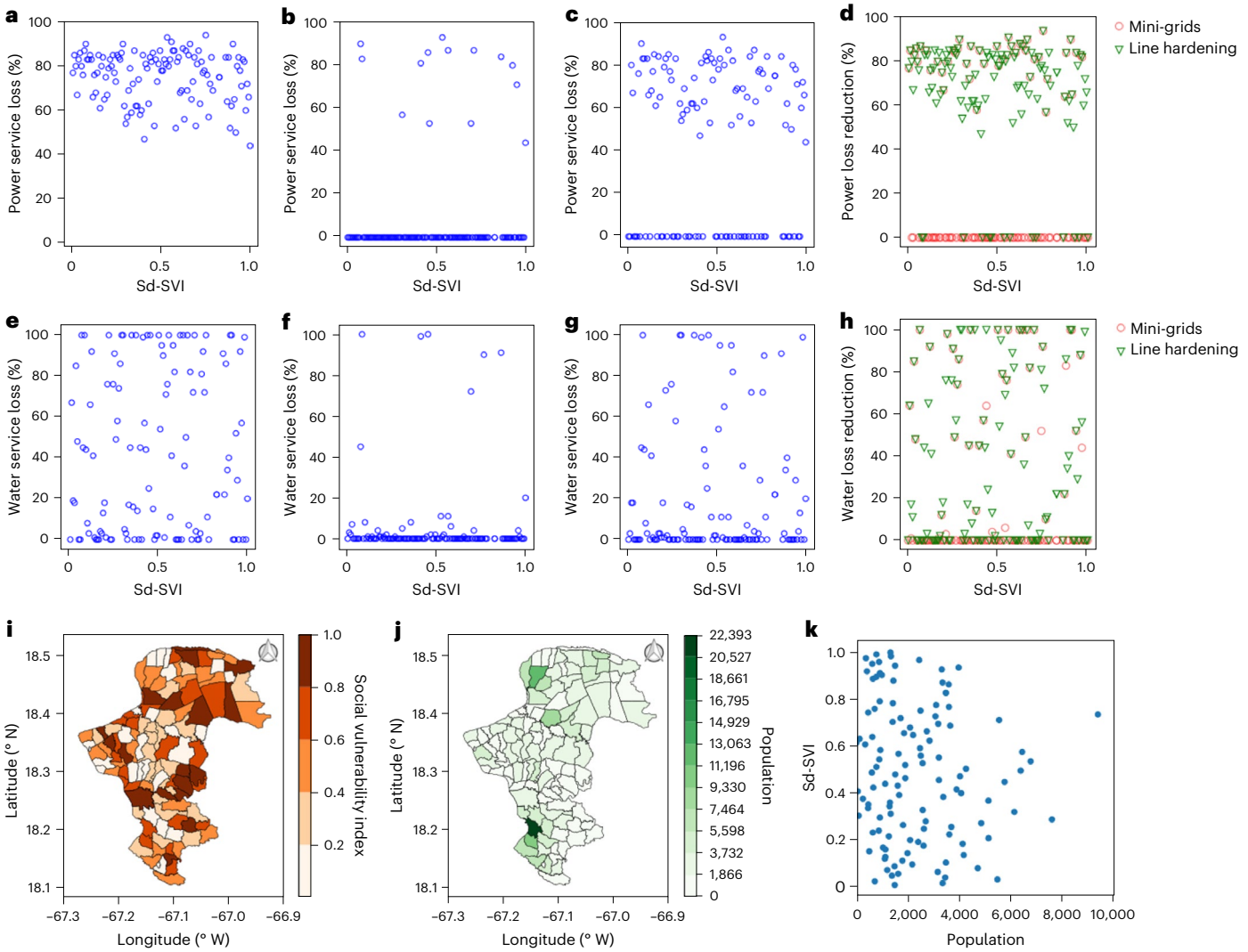

Fig. 6 | Socio-technical analysis. a, Observed power service loss in county subdivisions of varying degrees of Sd-SVI under baseline infrastructure scenario. **b**, Expected power service loss in county subdivisions of varying degrees of Sd-SVI under lines hardening infrastructure scenario. **c**, Expected power service loss in county subdivisions of varying degrees of Sd-SVI under mini-grids scenario. **d**, The effectiveness of hardening and mini-grids by depicting the level of power outage induced by the baseline infrastructure can be reduced with these system upgrades. **e**, Observed water service loss in county subdivisions of varying degrees of Sd-SVI under baseline infrastructure scenario. **f**, Expected water service loss in county subdivisions of varying degrees of Sd-SVI under lines hardening infrastructure scenario. **g**, Expected water service loss in county subdivisions of varying degrees of Sd-SVI under mini-grids scenario. **h**, The effectiveness of hardening and mini-grids by depicting the level of water outage induced by the baseline infrastructure can be reduced with these system upgrades. **i**, Sd-SVI at county subdivision level. **j**, Population count at county subdivision level. **k**, Scatter plot of Sd-SVI versus population.

We used this index to identify how the potential system upgrades impact the vulnerable communities and prioritized the upgrade option, which could improve the condition of the most vulnerable communities.

Results of socio-technical vulnerability and service loss

This work executed a coupled power–water vulnerability analysis for several hardening scenarios of the interconnected infrastructure, enabling comparative studies with the social burden resulting from power and water loss service. Figure 6a–h shows the expected water and power service loss for each county subdivision (total 119) in western Puerto Rico as a function of the Sd-SVI of that subdivision. Three scenarios are compared: (1) H-Maria equivalent incident as the baseline; (2) power lines hardening scenario; and (3) energy mini-grids scenario. Each point on the graphs in Fig. 6a–h represents one county subdivision. In this baseline (H-Maria) scenario, all county subdivisions experienced a loss of service, regardless of their Sd-SVI status. Altogether 100% of the population was at risk of power outages and 83% of the population was at risk of water outages. However, hardening the transmission lines improves the condition dramatically, where only 14 out of 119 county subdivisions will experience power outages, and some degree of water outage will occur in 34 county subdivisions, making a total of 13% of the study area population with power loss and 34% of the people with water loss. On the other hand, when considering the mini-grids upgrade scenario, 73 out of 119 subdivisions will face power loss and 64 subdivisions will face water service loss. Consequently, 58% of the residents in the area of study experience power outages and 60% experience water outages. Therefore, service loss is much lower by hardening transmission lines than by introducing the mini-grids proposed by the IRP.

Table 2 shows the affected population in the three different scenarios. Our study area of the western part of the island considers over 300,000 people, where more than one-third population falls into the high to very high socially vulnerable category with Sd-SVI

Table 2 | Affected population of different social vulnerability groups under current, hardening and mini-grids scenarios

Social vulnerability	Sd-SVI range	Number of county subdivisions	Population	Percent of population affected by service loss					
				Baseline infrastructure		Hardening		Mini-grids	
				Power	Water	Power	Water	Power	Water
Very low	0.0–0.2	25	57,625	100%	84.5%	10.7%	54.4%	60.8%	72.1%
Low	0.2–0.4	25	63,685	100%	82.9%	2.0%	25.4%	51.1%	43.8%
Medium	0.4–0.6	25	77,271	100%	79.5%	22.4%	46.5%	50.4%	57.5%
High	0.6–0.8	24	75,700	100%	85.2%	11.5%	18.7%	68.6%	69.2%
Very high	0.8–1.0	20	35,513	100%	84.6%	24.8%	23.1%	60.7%	58.6%

over 0.6. When subject to a similar level of service disruption, these highly vulnerable communities will suffer more than others. Results indicate that the power lines hardening option has a differential benefit to the highly endangered population.

In the lines hardening upgrade option, in an H-Maria-type event, 12% of the very high vulnerable population will lose power and 19% will lose water, while 11% of the very low vulnerable population will lose power and 54% will lose water.

Ultimately, the coupled power–water methodology was used to test the effect of different critical infrastructure upgrades in power and water delivery. In the case of Puerto Rico, we found that the proposed use of mini-grids was less effective than lines hardening in reducing hurricane-induced water and power service loss. This is probably due to the fact that mini-grids will still rely on the transmission system to reach distribution points. Additionally, many vulnerable communities are located in isolated areas, away from power generation. Compared to mini-grid solutions, hardening transmission lines reduces service outages overall and promotes greater social equality by minimizing service disruption for vulnerable populations.

Conclusions

Critical infrastructure is highly reliant on a functioning power system, and any disruption to the power supply can result in a service outage for other essential components, such as water. This can have severe consequences for the well-being of communities, especially during extreme natural events. This study has demonstrated a coupled water–power modelling approach for infrastructure vulnerability analysis, taking the impact of H-Maria on western Puerto Rico as a case study.

Our findings indicate that the impact of combined service disruption on different communities varies based on social vulnerability. In the case of system upgrades, it is crucial to incorporate community social burdens so that upgrade options can provide equity in service delivery to reduce vulnerability. This study demonstrated methods of developing service disruption metrics for each service upgrade scenario and incorporated those metrics with the social burden to quantify how each system upgrade would affect vulnerable communities.

For the power infrastructure upgrades, the study found that the power transmission lines hardening option could make the system far more resilient during a hurricane event and provide more equitable service to all communities compared to the mini-grids proposed by the IRP, which was suggested as a government policy option for reduced vulnerability.

This study presented a highly transferable and applicable methodology and analysis technique that can be applied to other areas of interest where essential services are disrupted due to natural disasters, such as power and water, where there are considerations for future upgrades on physical infrastructure assets to reduce vulnerability.

Future work could involve incorporating a recovery measure into both the power and water modelling and conducting a comprehensive analysis of the social adaptive capacity. This would provide an opportunity to examine the resilience of the system and the community in response to new critical infrastructure upgrades.

Methods

Power tower failure model

The PTF is a Random Forest model[54], trained with power tower characteristics and weather conditions to predict the failure in the power towers. The data used was provided by Puerto Rico Power Authority for the towers' characteristics and an H-Maria Weather Research and Forecasting model simulation[55] for the weather variables. Characteristics such as tower type, material, location of the tower, along with maximum wind speed, duration of high wind speed, rainfall, elevation and land cover were used to train the model. Moreover, using a fivefold cross-validation and 300 replicates of the model, we found the optimal parameters for the PTF to be 200 trees with a maximum depth of ten and a maximum of six features considered for splitting each node. Montoya et al. provide more details on the configuration and variables used for the PTF model[27].

The power network model

The PNM developed by Carvalhaes et al.[28] is a simple network flow model composite of all the generation centres and transmission lines in Puerto Rico. The model uses the generator capacities and the transmission capacity of the non-failed lines to estimate the flow over each line and the power supplied at each county. The model is sensitive to the damage to each of the modelled components. In this case, we focused on the impact that the failure of the transmission lines had on the power delivery to the customers. Such impact is quantified on a per-county basis as the count of people without power. Additionally, the PTF is used to forecast the damage to the transmission structures, and then the result is aggregated on a line-by-line basis. Consequently, the per-line damage aggregation is used as the input for the PNM. Multiple instances of the coupled models were executed to find an ideal threshold to convert from the percentage of damaged structures to a binary value of failure in each transmission line. We found that H-Maria power loss was better replicated when the threshold was set to 1% of failed structures. Therefore, a transmission line with more than 1% of damaged towers is reported as failed in the PNM.

Water distribution model

The initial water distribution model (WDM) from PRASA was a very detailed hydraulic model that included the location of pipelines, tanks, potable pump stations, intake facilities and junctions. It should be mentioned that a Python script was developed to adjust the demand of each junction, considering the nearby customers around it and the location of each of the junctions, then the updated junction demand was imported to the Infowater model. As a result, Fig. 1e shows the distribution of customer demand per municipal and county subdivisions.

Flooding modelling

The development of the hydrologic models for the four watersheds had a resolution of 100 metres, and they were based on the same

methodology used by Mejia-Manrique et al.[35]. The GSSHA model relies on the Digital Elevation Model of 10 metres, land-use land cover dataset and soil information. In addition, the Light Detection and Ranging data from the United States Geological Survey (USGS) was used to get the cross-section of the river channel by making use of geographic information systems (GIS) and a Python script. As noted by Mejia-Manrique et al., the calibration process of the parameters can be done by using the Secant Levenberg–Marquardt method, which is an enhancement version of the Levenberg–Marquardt method[35,56] available in GSSHA. It should be mentioned that the NTP (Storm Total Precipitation) Level 3 product from the Next Generation Radar was used to acquire the spatial and temporal distribution of the rainfall for the calibration and validation events shown in Table 1. Please refer to Mejia-Manrique et al. for more details on methodology[35]. In the case of the Yagüez watershed, We compared the most representative soil type and land-use land cover class between the Yagüez watershed and the area above the USGS stream discharge station of the Añasco Watershed, which corresponds to the area of the Añasco watershed that was used in the calibration process (Upstream Añasco watershed), and we concluded that the most representative categories coincided, which are mixed forest and clay, for the land-use land cover and soil class, respectively; with the following percentages for the mixed forest, with 77.4% and 69.8% for upstream Añasco and Yagüez watersheds, respectively. And for clay, with 89.9% and 77.5% for the upstream Añasco and Yagüez watersheds, respectively. Moreover, the potable pump water from the WDM was overlaid on each of the flooding maps to see which were affected by flooding. Furthermore, the potable water pumps from the WDM were overlaid on the flood maps to determine which were affected. Critical infrastructures were considered to be damaged or destroyed by flood depths greater or equal to 20 cm.

Coupling modelling

According to the power network model, the potable water pump stations were turned off based on the counties that did not have electricity, in addition, the water level from tanks was decreased for those tank facilities that depend on a potable water pump station. These data were transferred to the WDM to run the simulation. It should be noted that the water and power model simulations were run in a steady state. Subsequently, the results were converted to a percentage of service level, as shown in Fig. 4. The power service loss was computed by subtracting a hundred percent from the percentage of change between the Lights at Night product from NASA (NTL) (equation (1)). In the case of the water service loss, it was determined by subtracting a hundred from the ratio between the total loss of supply and the total supply multiplied by a hundred (equation (2)).

$$\text{Power Service Loss}\,(\%) = 100 - \frac{\text{NTL}_{\text{Base}} - \text{NTL}_{\text{After}}}{\text{NTL}_{\text{Base}}} \times 100 \quad (1)$$

$$\text{Water Service Loss}\,(\%) = \frac{\text{Total loss of supply}\,(\text{m}^3\,\text{d}^{-1})}{\text{Total supply}\,(\text{m}^3\,\text{d}^{-1})} \times 100 \quad (2)$$

Social analysis

For policy or systems upgrade recommendations to reduce the community's vulnerability and human suffering, it is necessary to consider social vulnerability. Here we formulated the social vulnerability index for power and water service disruption (Sd-SVI) at the county subdivision level for the western part of the island.

In Sd-SVI, we incorporated 12 variables from three themes. The attributes included in the Sd-SVI are as follows:

Theme 1 (socioeconomic status):

- Poverty: percent households living below the poverty line
- Unemployment: percent of the unemployed population
- Income: median household income (inverted for vulnerability calculation)
- Education: percent population having no high school diploma

Theme 2 (household composition):

- Aged population: percent population over 64
- Young population: percent population less than 18
- Disability: percent population over five years and disabled
- Single-parent households: percent of single-parent households

Theme 3 (accessibility)

- Vehicles: percent households with no vehicle
- Hospital: distance to the closest hospital
- Supermarket: distance to the closest supermarket
- Road density: density of road network (m km^{-2})

We collected socioeconomic and household composition data from American Community Survey[57]. We obtained road data and information on supermarket and hospital locations from OpenStreetMap[58]. To estimate the accessibility to supermarkets and hospitals, we calculated the distance of the nearest hospitals and supermarkets from the centroid of each county subdivision.

Even though Sd-SVI was built on CDC SVI, it is worth noting that we did not include attributes relating to household crowdedness and minority status in Sd-SVI, even though these two themes were included in CDC SVI[19]. Household crowdedness can contribute to vulnerability during disaster evacuations that do not involve power and water service interruptions. In the case of minorities, the demography of Puerto Rico is different from the US mainland, with a predominantly Hispanic population of approximately 98.8% (ref. 59). Therefore, minority status is not a relevant factor in vulnerability and service outages.

To construct Sd-SVI, we followed the method of CDC SVI[19]. All 12 variables (Table 2), except for per capita income and road density, were arranged in descending order across all 119 barrios in the study area. This was done because a higher value for these variables indicates a greater vulnerability. Conversely, per capita income and road density were arranged in ascending order because a higher value indicates lesser vulnerability. After ranking the variables, a percentile rank was calculated for each barrio across each variable.

$$\text{Percentile Rank} = \frac{(\text{Rank} - 1)}{(N - 1)} \quad (3)$$

To compute the percentile rank, equation (3) was used, where 'Rank' represents the rank of the county subdivision's score for a particular variable and N denotes the total number of barrios in the study area. Furthermore, we computed the percentile rank of each county subdivision for each of the three domains by adding up the percentile ranks of the variables in that specific domain. Ultimately, we determined an overall percentile rank for each county subdivision by summing up the percentile rankings of the three domains.

Limitations

This study is limited to a steady state socio-technical vulnerability analysis, where the effect of recovery is not considered in the analysis. As a result, the study does not explicitly measure social adaptive capacity or resilience. While the Sd-SVI index captures various attributes contributing to vulnerability, it may not fully capture a community's ability to adapt to or recover from these disruptions.

Data availability

The datasets generated and/or analysed during the current study are available in the Zenodo repository https://doi.org/10.5281/zenodo.7388021.

References

1. Bennett, J. A. et al. Extending energy system modelling to include extreme weather risks and application to hurricane events in Puerto Rico. *Nat. Energy* **6**, 240–249 (2021).
2. Yates, D. et al. Stormy weather: assessing climate change hazards to electric power infrastructure: a Sandy case study. *IEEE Power Energy Mag.* **12**, 66–75 (2014).
3. Schmeltz, M. T. et al. Lessons from Hurricane Sandy: a community response in Brooklyn, New York. *J. Urban Health* **90**, 799–809 (2013).
4. Pasch, R. J., Penny, A. B. & Berg, R. *National Hurricane Center Tropical Cyclone Report Hurricane Maria (AL152017) 16–30 September 2017*. National Hurricane Center (2019).
5. Birk Jones, C., Bresloff, C. J., Darbali-Zamora, R., Lave, M. & Aponte Bezares, E. E. Geospatial assessment methodology to estimate power line restoration access vulnerabilities after a hurricane in Puerto Rico. *IEEE Open Access J. Power Energy* https://doi.org/10.1109/OAJPE.2022.3191954 (2022).
6. Lu, D. & Alcantara, C. After Hurricane Maria, Puerto Rico was in the dark for 181 days, 6 hours and 45 minutes. *The Washington Post*. April 4, 2018 (2018).
7. Mahzarnia, M., Moghaddam, M. P., Baboli, P. T. & Siano, P. A review of the measures to enhance power systems resilience. *IEEE Syst. J.* **14**, 4059–4070 (2020).
8. Panteli, M., Trakas, D. N., Mancarella, P. & Hatziargyriou, N. D. Power systems resilience assessment: hardening and smart operational enhancement strategies. *Proc. IEEE* **105**, 1202–1213 (2017).
9. Bagheri, A., Zhao, C., Qiu, F. & Wang, J. Resilient transmission hardening planning in a high renewable penetration era. *IEEE Trans. Power Syst.* **34**, 873–882 (2019).
10. Elizondo, M. A. et al. *Risk-Based Dynamic Contingency Analysis Applied to Puerto Rico Electric Infrastructure* (US Department of Energy, 2020); https://doi.org/10.2172/1771798
11. Boyle, E. et al. Social vulnerability and power loss mitigation: a case study of Puerto Rico. *SSRN Electron. J.* https://doi.org/10.2139/SSRN.3838896 (2021).
12. Kwasinski, A., Andrade, F., Castro-Sitiriche, M. J. & O'Neill-Carrillo, E. Hurricane Maria effects on Puerto Rico electric power infrastructure. *IEEE Power Energy Technol. Syst. J.* **6**, 85–94 (2019).
13. O'Neill-Carrillo, E. & Irizarry-Rivera, A. How to harden Puerto Rico's grid against hurricanes. *IEEE Spectr.* **56**, 42–48 (2019).
14. Siddiqi, A., Kajenthira, A. & Anadón, L. D. Bridging decision networks for integrated water and energy planning. *Energy Strategy Rev.* **2**, 46–58 (2013).
15. Roni, M. S. et al. Integrated water–power system resiliency quantification, challenge and opportunity. *Energy Strategy Rev.* **39**, 100796 (2022).
16. Zuloaga, S. & Vittal, V. Integrated electric power/water distribution system modeling and control under extreme mega drought scenarios. *IEEE Trans. Power Syst.* **36**, 474–484 (2021).
17. Pant, R., Thacker, S., Hall, J. W., Alderson, D. & Barr, S. Critical infrastructure impact assessment due to flood exposure. *J. Flood Risk Manage.* **11**, 22–33 (2018).
18. Dargin, J., Berk, A. & Mostafavi, A. Assessment of household-level food–energy–water nexus vulnerability during disasters. *Sustainable Cities Soc.* **62**, 102366 (2020).
19. Flanagan, B. E., Gregory, E. W., Hallisey, E. J., Heitgerd, J. L. & Lewis, B. A social vulnerability index for disaster management. *J. Homeland Secur. Emerg. Manage.* **8**, 1–8 (2011).
20. Cutter, S. L., Mitchell, J. T. & Scott, M. S. Revealing the vulnerability of people and places: a case study of Georgetown County, South Carolina. *Ann. Assoc. Am. Geogr.* **90**, 713–737 (2000).
21. Emrich, C. T. & Cutter, S. L. Social vulnerability to climate-sensitive hazards in the Southern United States. *Weather Clim. Soc.* **3**, 193–208 (2011).
22. Blaikie, P., Cannon, T., Davis, I. & Wisner, B. At risk: natural hazards, people's vulnerability and disasters. *Risk* https://doi.org/10.4324/9780203974575 (2005).
23. West, J., Riosmena, F. & Thomas, K. Comparing social vulnerability and population loss in Puerto Rico after Hurricane Maria. M.A. thesis, University of Colorado Boulder. 1–5 (2022).
24. Wood, E., Sanders, M. & Frazier, T. The practical use of social vulnerability indicators in disaster management. *Int. J. Disaster Risk Reduct.* **63**, 102464 (2021).
25. Bergstrand, K., Mayer, B., Brumback, B. & Zhang, Y. Assessing the relationship between social vulnerability and community resilience to hazards. *Social Indic. Res.* **122**, 391–409 (2015).
26. Spielman, S. E. et al. Evaluating social vulnerability indicators: criteria and their application to the Social Vulnerability Index. *Nat. Hazards* **100**, 417–436 (2020).
27. Montoya-Rincon, J. P., Gonzalez, J. E. & Jensen, M. P. Evaluation of Transmission Line Hardening Scenarios using a Machine Learning Approach. ASCE-ASME Journal of Risk and Uncertainty in Engineering Systems Part B: Mechanical Engineering https://doi.org/10.1115/1.4063012 (2023).
28. Carvalhaes, T. et al. A simulation framework for service loss of power networks under extreme weather events: a case of Puerto Rico. In *IEEE International Conference on Automation Science and Engineering* 1532–1537 https://doi.org/10.1109/CASE48305.2020.9216849 (2020).
29. Román, M. O. et al. NASA's Black Marble nighttime lights product suite. *Remote Sens. Environ.* https://doi.org/10.1016/j.rse.2018.03.017 (2018).
30. Montoya-Rincon, J. P. et al. On the use of satellite nightlights for power outages prediction. *IEEE Access* **10**, 16729–16739 (2022).
31. Román, M. O. et al. Satellite-based assessment of electricity restoration efforts in Puerto Rico after Hurricane Maria. *PLoS ONE* **14**, e0218883 (2019).
32. Azad, S. & Ghandehari, M. A study on the association of socioeconomic and physical cofactors contributing to power restoration after Hurricane Maria. *IEEE Access* **9**, 98654–98664 (2021).
33. Wang, Z. et al. Monitoring disaster-related power outages using NASA Black Marble nighttime light product. *Int. Arch. Photogramm. Remote Sens. Spat. Inf. Sci.* **42**, 1853–1856 (2018).
34. Innovyze Store *InfoWater* (Innovyze Store, 2021); https://store.innovyze.com/WaterDistribution/InfoWater?cclcl=en_US
35. Manrique, S. A. M., Harmsen, E. W., Khanbilvardi, R. M. & González, J. E. Flood impacts on critical infrastructure in a coastal floodplain in western Puerto Rico during Hurricane María. *Hydrology* **8**, 104 (2021).
36. US Army Corps of Engineers *Gridded Surface Subsurface Hydrologic Analysis* (US Army Corps of Engineers, 2022); https://www.erdc.usace.army.mil/Media/Fact-Sheets/Fact-Sheet-Article-View/Article/476714/gridded-surface-subsurface-hydrologic-analysis/#:~%7B%7D:text=GSSHA
37. Giovanni-Prieto, M. *Development of a Regional Integrated Hydrologic Model for a Tropical Watershed*. MSc thesis, Univ. of Puerto Rico, Mayaguez Campus (2007).
38. Rojas-González, A. M. *Flood Prediction Limitations in Small Watersheds with Mountains Terrain and High Rainfall Variability*. Ph.D dissertation, Univ. of Puerto Rico, Mayaguez Campus (2012).
39. Silva-Araya, W. F., Santiago-Collazo, F. L., Gonzalez-Lopez, J. & Maldonado-Maldonado, J. Dynamic modeling of surface runoff and storm surge during hurricane and tropical storm events. *Hydrology* **5**, 13 (2018).
40. Moriasi, D. N., Gitau, M. W., Pai, N. & Daggupati, P. Hydrologic and water quality models: performance measures and evaluation criteria. *Trans. ASABE* **58**, 1763–1785 (2015).

41. Yuan, H., Zhang, W., Zhu, J. & Bagtzoglou, A. C. Resilience assessment of overhead power distribution systems under strong winds for hardening prioritization. *ASCE-ASME J. Risk Uncertainty Eng. Syst. Part A Civ. Eng.* **4**, 04018037 (2018).
42. Salman, A. M., Li, Y. & Stewart, M. G. Evaluating system reliability and targeted hardening strategies of power distribution systems subjected to hurricanes. *Reliab. Eng. Syst. Saf.* **144**, 319–333 (2015).
43. Wang, Y., Rousis, A. O. & Strbac, G. On microgrids and resilience: a comprehensive review on modeling and operational strategies. *Renew. Sustain. Energy Rev.* **134**, 110313 (2020).
44. Aros-Vera, F., Gillian, S., Rehmar, A. & Rehmar, L. Increasing the resilience of critical infrastructure networks through the strategic location of microgrids: a case study of Hurricane Maria in Puerto Rico. *Int. J. Disaster Risk Reduct.* **55**, 102055 (2021).
45. *Puerto Rico Integrated Resource Plan 2018-2019* Vol. 1 (Siemens Industry, 2019); https://energia.pr.gov/wp-content/uploads/sites/7/2019/06/2-IRP2019-Main-Report-REV2-06072019.pdf
46. Zamzam, A. S., Dall'Anese, E., Zhao, C., Taylor, J. A. & Sidiropoulos, N. D. Optimal water–power flow-problem: formulation and distributed optimal solution. *IEEE Trans. Control Network Syst.* **6**, 37–47 (2019).
47. Shinozuka, M. et al. Resilience of integrated power and water systems. *Seism. Eval. Retrofit Lifeline Syst.* **65**, 65–86 (2003).
48. Dugan, J., Byles, D. & Mohagheghi, S. Social vulnerability to long-duration power outages. *Int. J. Disaster Risk Reduct.* **85**, 103501 (2023).
49. Tarling, H. A. Comparative Analysis of Social Vulnerability Indices: CDC's SVI and SoVI. *Division of Risk Management and Societal Safety, Lund University* (2017).
50. Cutter, S. L., Boruff, B. J. & Shirley, W. L. Social vulnerability to environmental hazards*. *Social Sci. Q.* **84**, 242–261 (2003).
51. Carvalhaes, T. et al. Integrating spatial and ethnographic methods for resilience research: a thick mapping approach for Hurricane Maria in Puerto Rico. *Ann. Am. Assoc. Geogr*. https://doi.org/10.1080/24694452.2022.2071200 (2022).
52. Chakalian, P. M., Kurtz, L. C. & Hondula, D. M. After the lights go out: household resilience to electrical grid failure following Hurricane Irma. *Nat. Hazards Rev.* **20**, 05019001 (2019).
53. Puerto Ricans at risk of waterborne disease outbreaks in wake of Hurricane Maria. *CBS News*. Oct 25, 2017 (2017).
54. Breiman, L. Random forests. *Mach. Learn*. https://doi.org/10.1023/A:1010933404324 (2001).
55. Pokhrel, R., Cos del, S., Montoya Rincon, J. P., Glenn, E. & González, J. E. Observation and modeling of Hurricane Maria for damage assessment. *Weather Clim. Extremes* https://doi.org/10.1016/j.wace.2021.100331 (2021).
56. Skahill, B. E., Charles, D. W. & Bagget, J. S. *A Practical Guide to Calibration of a GSSHA Hydrologic Model Using ERDC Automated Model Calibration Software – Effective and Efficient Stochastic Global Optimization. U.S. Army Engineer Research and Development Center* (2012).
57. *2014–2018 ACS 5-year Estimates* (US Census Bureau, 2018); https://www.census.gov/programs-surveys/acs/technical-documentation/table-and-geography-changes/2018/5-year.html
58. OpenStreetMap contributors. *Planet Dump. OpenStreetMap* (2017).
59. Tormos-Aponte, F., García-López, G. & Painter, M. A. Energy inequality and clientelism in the wake of disasters: from colorblind to affirmative power restoration. *Energy Policy* **158**, 112550 (2021).

Acknowledgements

The authors gratefully acknowledge the financial support received by the US National Science Foundation under grant CBET-1832678, the National Science Foundation Program for Critical Resilient Interdependent Infrastructure Systems and Processes titled 'Integrated Socio-Technical Modeling Framework to Evaluate and Enhance Resiliency in Islanded Communities' under award 1832678.

Author contributions

J.P.M.-R.: data collection, formal analysis, writing, review and editing. S.A.M.-M.: data collection, formal analysis, writing, review and editing. S.A.: data collection, formal analysis, writing, review and editing. M.G.: funding acquisition, review and editing. E.W.H.: funding acquisition, review and editing. R.K.: funding acquisition and review. J.E.G.-C.: funding acquisition, project lead, review and editing.

Competing interests

The authors declare no competing interests.

Additional information

Correspondence and requests for materials should be addressed to Juan P. Montoya-Rincon or Said A. Mejia-Manrique.

Peer review information *Nature Energy* thanks the anonymous reviewers for their contribution to the peer review of this work.

Reprints and permissions information is available at www.nature.com/reprints.

Publisher's note Springer Nature remains neutral with regard to jurisdictional claims in published maps and institutional affiliations.